ISSN: 0975-8585

Research Journal of Pharmaceutical, Biological and Chemical Sciences

A short review on hybrid PVDF-nanomaterials based super-hydrophobic coatings

Prasad G, and Anand Prabu A*.

Centre for Nanomaterials, Department of Chemistry, School of Advanced Sciences, Vellore Institute of Technology University, Vellore 632 014, India.

ABSTRACT

Research into the fabrication of extremely hydrophobic surfaces began many decades ago, and the motivation to prepare such a surface arose after the discovery of dual hierarchal structure in lotus leaf. It was only at the start of this decade that the term super-hydrophobicity (SHB) appeared in literature, and since then, the interest in SHB surfaces has grown exponentially in the recent years. In this review, our aim is to explore the latest developments in the field of polyvinylidene fluoride (PVDF) nanocomposite based super-hydrophobic coatings (SHBCs). The discussion will focus on the PVDF characteristics, nanomaterials used, sample preparation parameters, morphological, spectral and water-contact angle measurements. The transition from super-hydrophobic to super-hydrophilic upon tweaking the polymer chain-dipole arrangements and polymer-nanomaterial interaction is also covered in this review. Moreover, some of the difficulties faced during the fabrication of SHCs and their future roadmap were also discussed.

Keywords: Polyvinylidene fluoride; nanomaterials; super-hydrophobicity; wetting; dipole orientation.

Corresponding author
Email id: anandprabu@vit.ac.in

ISSN: 0975-8585

INTRODUCTION TO SURFACE WETTABILITY

In the past decades, bioinspired surfaces with super-hydrophobicity that is one of the extreme states of surface wettability have been intensively explored and accelerated by discoveries of super-wetting phenomena in nature. Several possible extreme states of super-wettability were disclosed in **Fig. 1 (**Wang et al. 2015**)**, including super-hydrophobic (SHB), super-hydrophilic (SHL), super-oleophilic (SOL), and super-oleophobic (SOB). When air is changed to water or oil, several possible extreme states appear: underwater super-oleophobic (WSOB), underwater super-oleophilic (WSOL), under oil super-hydrophobic (OSHB), and under oil super-hydrophilic (OSHL). Those terms, going far beyond new terminologies, have dramatically accelerated the development of new surface technologies and deepen the understanding of fundamental knowledge of wettability.

The surface wettability is measured by the contact angle (CA) which a water droplet forms when it is put on a surface. Self-cleaning surfaces exhibit special non-wetting properties owing to a water contact angle >150°. On a slippery surface, the water droplets do not penetrate into the asperities of surface, and the interactions with the surfaces are lowered. On the other hand, SHB surfaces show high sticky behavior and exhibit high water contact angle (>150°). Due to the high roughness, water droplets are less prone to roll off on them, and instead penetrate into cavities of surface. The high roughness increases the contact area, and as consequence, the liquid–solid interactions are increased.

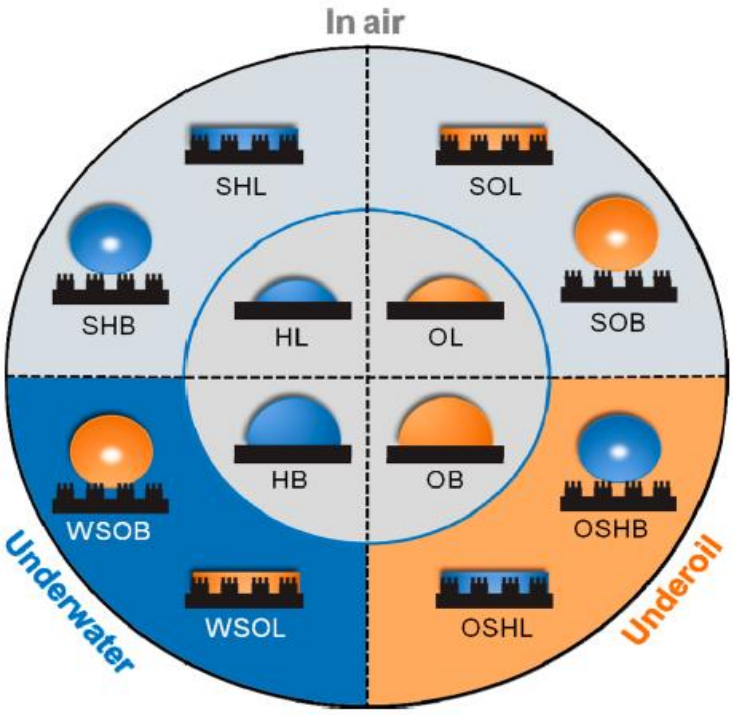

Fig. 1. Possible extreme states of surface wettability (Wang et al. 2015).

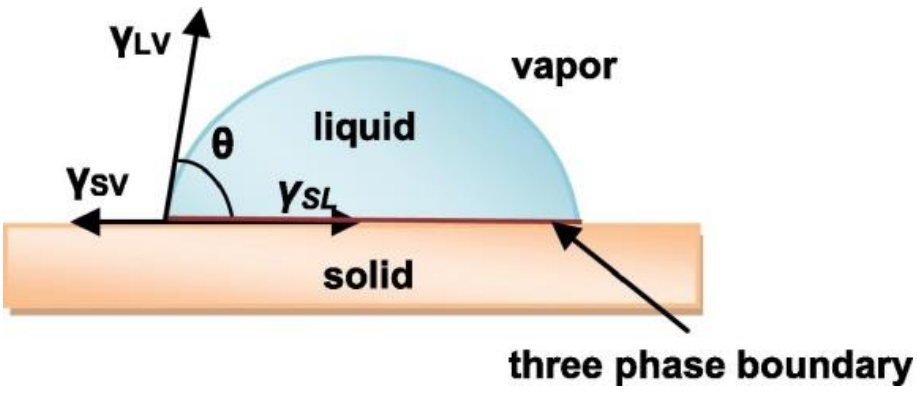

ISSN: 0975-8585

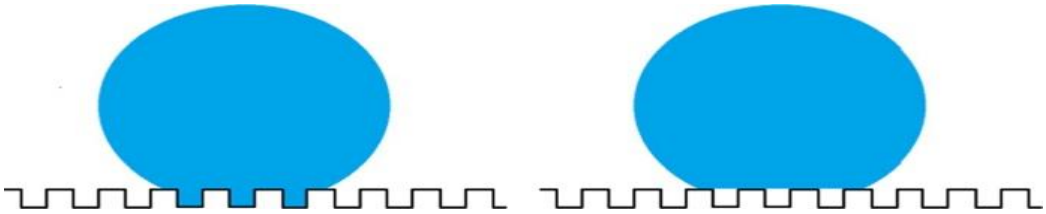

Fig. 2. (Top) Diagram showing the forces at the three-phase contact line of a liquid droplet on a solid; and (Bottom) Behavior of a liquid droplet on a rough surface: Left, Wenzel state and right, Cassie-Baxter state (Celia et al. 2013).

CA can be defined as the tangent angle of the liquid–vapor interface at the three-phase boundary (**Fig. 2, Top**). For a smooth surface, the contact angle is described by the Young Eq. (1). where γ_{LV} relates to the interfacial tension between liquid and vapor, γ_{SL} is the interfacial tension between solid and liquid, and γ_{SV} is the interfacial tension between solid and vapor.

$$\cos\theta = \frac{(\gamma_{SV} - \gamma_{SL})}{(\gamma_{LV})} \quad \text{……(1)}$$

For CA <90°, the surface is conventionally described as hydrophilic, if the CA varies between 90° and 150°, the surface is hydrophobic, and if water CA is >150°, the surface is SHB. HB surfaces can be enhanced to SHB by addition of roughness or by a certain type of morphology. Two models have been elaborated which describe the behavior of a droplet on rough hydrophobic surfaces (**Fig. 2, Bottom**). According to the 1st model, the droplet maintains contact with the surface and penetrates the asperities, and the surface contact area is increased (the Wenzel case). In the 2nd model, the droplet is suspended on the asperities, and it rests on a composite phase made of both solid–liquid and solid–vapor interfaces (the Cassie-Baxter case). For many surfaces, a transition from Cassie-Baxter to Wenzel state was observed. Many factors can determine this change such as surface heterogeneity, both chemical heterogeneity and roughness, and the interaction at the contact line seems to play a crucial role in giving rise to adhesion hysteresis. The self-cleaning property is associated with a low CA hysteresis (usually <10°) and low sliding angle, SA (Celia et al. 2013).

Much progress in the field of SHBs happened when Barthlott and Neinhuis (1997) revealed that the self-cleaning property of lotus leaves was caused by the micro-scaled papillae and the epicuticular wax, providing a mono-microstructure model. Subsequently, Feng et al. (2002) disclosed micro- and nanoscaled hierarchical structures on the lotus leaf surface, i.e., branch-like nanostructures on the top of micropapillae, which result in the SHB behavior. Their mimicking study by using aligned carbon nanotube array further demonstrated that nanostructures can induce the high CA of SHB surfaces and multiscale structures can effectively reduce the SA. Thus, the origin of SHB of a lotus leaf becomes clear from a mono-scaled model of microstructures to a dual-scaled model of hierarchical structures (WCA >150^{o}). These studies on the lotus leaf activated the field of wettability from surface chemistry, biomimetic study, fundamental theory, and material science. In the following decade, a mass of surfaces with super-wettability that have been fabricated have shown promising potential applications in self-cleaning, anti-biofouling, anti-ice, anti-fogging, oil/water separation, smart membrane, sensor, microfluidic devices, to name a few.

Approaches towards Creating SHB Surfaces

The wettability of solid surface results not only from the chemical composition of a surface but also from its morphology or roughness. In the animal kingdom, the anti-wetting properties have also been developed and are correlated with some special functionality. The SHB and the water repellent properties also allow some water-walking insect to float and to move on water. Concerning the morphology, the cuticles are formed by hairs, scales, and regions where WCA can vary. The legs in particular present a high density of micro-sized hairs, named macrotrichia, that are covered by grooves. This particular structure allows the arthropod to float on the water surface. The highest WCA of a water skater leg were measured to reach 167^{o}. Actually, the SHB was attained owing to the double hierarchical structure of leg surface. Moreover, the orientation of hairs respect to the water surface and the presence of grooves seem to play an important role in the thrust generation and propulsion (**Fig. 3**). The strategies developed by these insects provided guidance to scientists to engineering biomimetic surfaces.

ISSN: 0975-8585

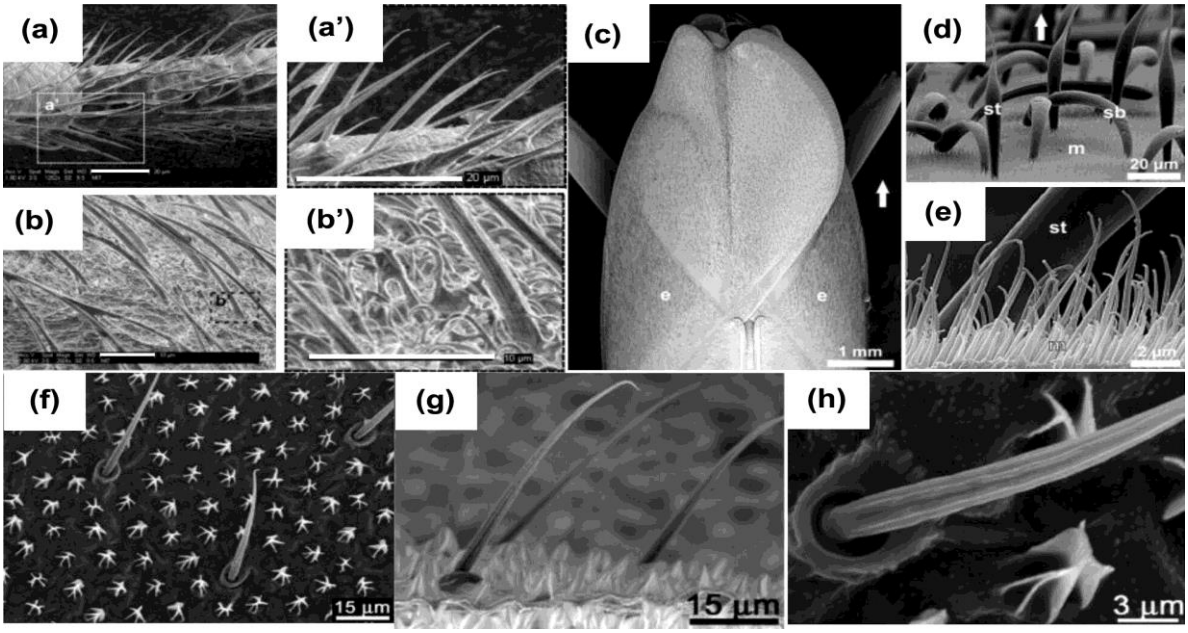

Fig. 3. SEM images of the hairy surface of the water treader Microvelia: (a) Leg hairs. In the magnified view (a'), the hair tips are bent inwards. (b) Body hairs: macrotrichia emerge from a tangle of microtrichia. (b') Makes clear the grooves on the macrotrichia. The scale bar is 20 µm in (a), 20 µm in (a'), 10 µm in (b), 10 µm in (b'), respectively (Bush et al. 2007); SEM micrographs of Notonecta glauca. Arrows point toward posterior. (c) Dorsal view of the posterior side of the elytra. (d) Differently shaped setae on the elytra: sharp-tipped setae and baseball bat-like setae stand above a very dense cover of microtrichia. (e) Lateral view of the microtrichia and setae. The heights of the microtrichia vary. e, elytra; m, microtrichia; sb, baseball bat-like setae; st, sharp-tipped setae; SEM images of the termite wing membrane surface Nasutiterems walkeri. (f) Topographical landscape showing hairs in sockets (macrotrichia) and star-shaped structures (micrasters) evenly spaced on the surface. (g) Topography (side view) hairs and micrasters on the wing membrane. (h) Higher resolution image showing the hair and micraster fine structure. Panels c–e reprinted with permission from Balmert et al. (2011). Panels f–h reprinted with permission from Watson et al. (2010).

There are two basic strategies to increase the CA and formation of more hydrophobic surface. One is to increase the surface roughness, which is known as the geometrical micro/nanostructure method. The rough surface was usually fabricated or modified with the low surface energy materials. In a rough surface, air is trapped between the water droplet and the surface, due to irregular surface, and the resulting CA hysteresis is very low. Another is to make change the surface chemistry, which is generally referred to as a chemical modifying method. Also, a SHB surface could be prepared via combination of these two procedures. It was believed that the hydrophobicity is connected to use of an appropriated roughness combined with a low surface energy material (Madaeni et al. 2013).

There are various approaches to create the SHB surfaces, including coating with fluoroalkylsilane, spin-coating of polytetrafluoroethylene (PTFE) on vertically-aligned carbon nanotubes (CNTs), self-assembling of special monolayer over thin films, plasma-enhanced chemical vapor deposition, plasma glow-discharge, ion-etching and plasma-modification, physical vapor deposition, sol-gel, mixing with silica or PTFE powders, nanofiber template-based extrusion method, electro-chemical deposition, laser-etching, spray-and-dry method, etc. (Madaeni et al. 2013). Some of the important materials used to make SHB surfaces are silicones, fluorocarbons, organic materials (polyethylene, polystyrene, etc.), and inorganic materials (ZnO and TiO_2). Fluoropolymers with their low surface energy are widely used for preparation of hydrophobic surfaces, such as water repellent fabric surfaces. However, it was reported that trifluoromethyl group (CF_3)-terminated flat surfaces with the lowest surface energy exhibited the highest WCA of 110–120^o which was much lower than 150^o. Therefore, SHB surfaces could not be achieved only by using fluorochemicals. The surface microstructures/nanostructures can be obtained by introducing inorganic nanosize particles such as SiO_2, TiO_2, ZnO, gold, silver and alumina nanoparticles, and CNTs. Recently, the hybrid materials had been extensively applied to fabricate SHB surfaces by the cooperation of low surface energy caused by organic materials and rough surface structures due to inorganic nanomaterials. Low cost nanosilica with higher strength and toughness, high temperature and corrosion resistant could be widely used as inorganic materials to prepare hybrid materials. Some researchers obtained SHB surfaces by physically mixing inorganic SiO_2 nanoparticles

and polymers. However, the main problem is the poor compatibility between inorganic nano SiO_2 materials and organic materials due to SiO_2 nanoparticle aggregation (Xu et al. 2014). By embedding hydrophobically modified fumed silica (HMFS) particles in polyvinylidene fluoride (PVDF) matrix, Basu and Paranthaman (2009) prepared PVDF-HMFS hybrid composite SHB coatings. Hsieh et al. (2011) fabricated water and oil repellency nanocoatings by well-mixing silica nanospheres and perfluoroalkyl methacrylic copolymers. Lakshmi et al. (2012) obtained sol–gel nanocomposite SHB coatings by incorporation of a perfluoroalkylmethacrylic copolymer in a hybrid sol–gel matrix containing fumed silica nanoparticles. Among the many materials available, we choose to review the usage of PVDF based SHB coatings, and in particular PVDF-nanomaterial hybrids based SHB coatings.

PVDF nanocomposite based SHB Coatings

Basu and Paranthaman (2009) reported the preparation of PVDF-hydrophobically modified fumed silica (HMFS) SHB coating using a simple spraying technique. In this method, PVDF is dissolved in DMF and silica, and their respective solutions were further dispersed in toluene. These two solutions were sprayed onto different substrates like glass, Alumina and PU coated Al. The effect of silica content on the hydrophobicity was also investigated. The blank PVDF solution exhibited a CA of about 95º and the SA >90º. With increasing addition of HMFS content, the CA increases and SA decreases as shown in **Table 1**, and the corresponding CA images are shown in **Fig. 4**.

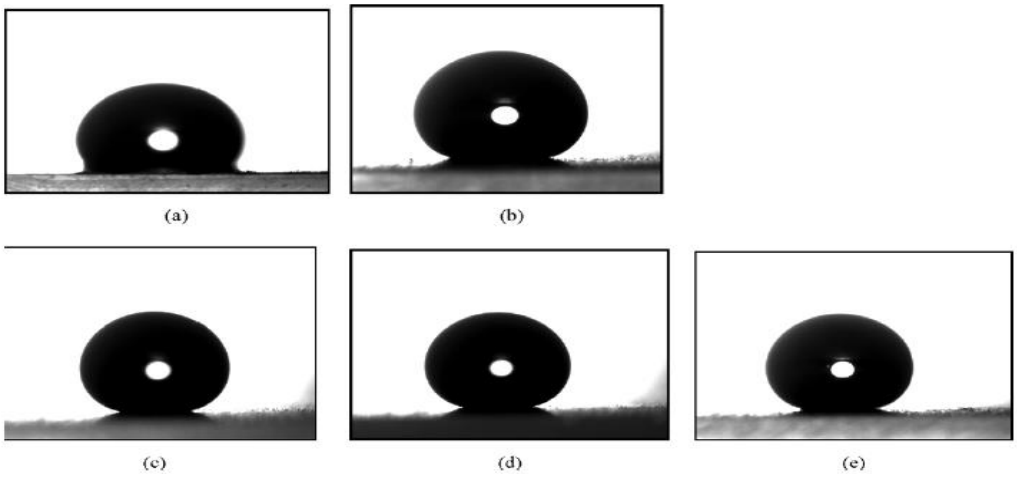

Fig. 4. Images of water drop on PVDF–HMFS coatings with different silica concentrations: (a) 33.37%, (b) 50%, (c) 60%, (d) 66.67% and (e) 71.42% (Basu and Paranthaman, 2009).

Table 1: Contact and sliding angles of PVDF–HMFS coatings with different filler concentrations

Concentration of HMFS silica (%)	PVDF to HMFS weight ratio	WCA (^{o})	SA (^{o})
0	–	95	>90
33.3	2:1	117	90
50	1:1	160	3
60	2:3	164	2
66.7	1:2	167	<1
71.4	2:5	168	<1

It was found that the PVDF: HMFS (1:1) composite coating prepared from a precursor aged for 3 days exhibited a porous structure with long nanofilaments (**Fig. 5c and d**). The composite coating with PVDF: HMFS (1:2) was rougher and displayed porous structure. When the precursor was ultrasonicated before spraying, SEM images showed micro-scale bumps interspersed with honeycomb-like structure (**Fig. 6c and d**). The areas surrounding the honeycomb contained silica particles. The aggregates of particle were smaller for coating prepared with ultrasonicated precursor. The bumps also had a microporous structure. In all the four cases, the composite coatings exhibited SHB irrespective of the differences in their microstructure. PVDF: HMFS (1:1) coating was not wetted after 6 h of immersion in water, and there was no change in WCA but an increase in SA

ISSN: 0975-8585

to about 158 was observed in the immersed area. The coating regained its SHB property after drying at R.T. PVDF: HMFS (1:2) coating was not wetted even after 30 h of immersion in water. But SA increased to 108 while there was no change in WCA. Drying at R.T. resulted in complete regaining of its SHB property. Composite coatings with higher silica concentration showed better water repellency than coatings with lower silica concentration.

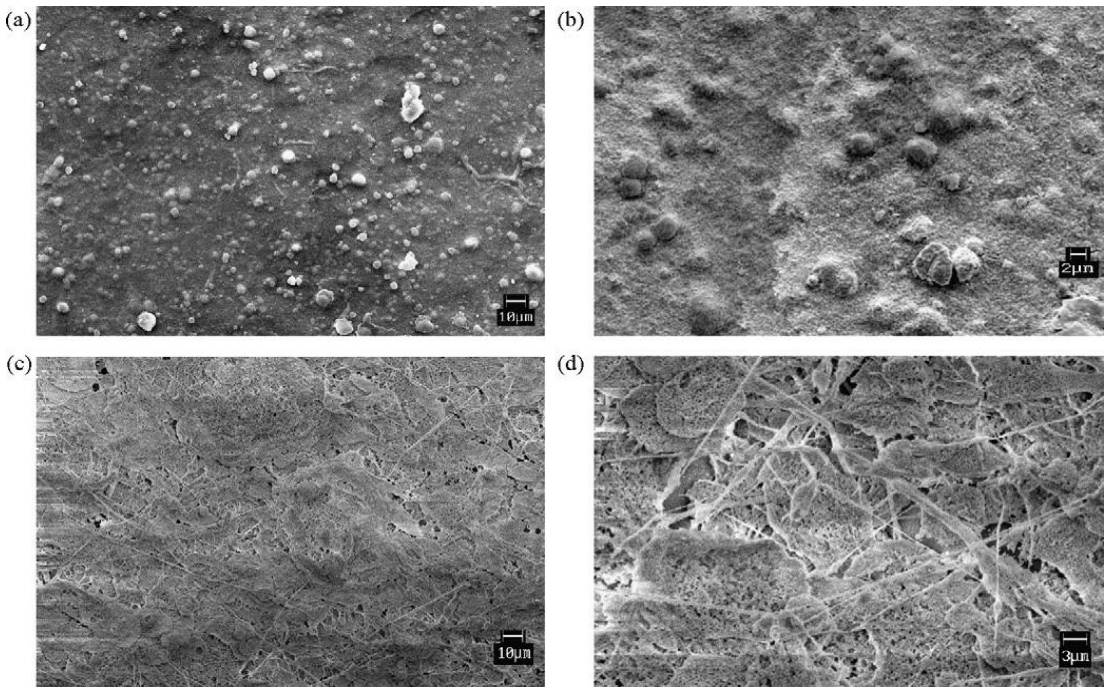

Fig. 5. SEM images of PVDF: HMFS (1:1) composite coatings prepared under different conditions: (a) with freshly mixed precursor, 500X; (b) higher magnification of (a); (c) after aging the precursor, 500X; and (d) higher magnification of (c) (Basu and Paranthaman, 2009).

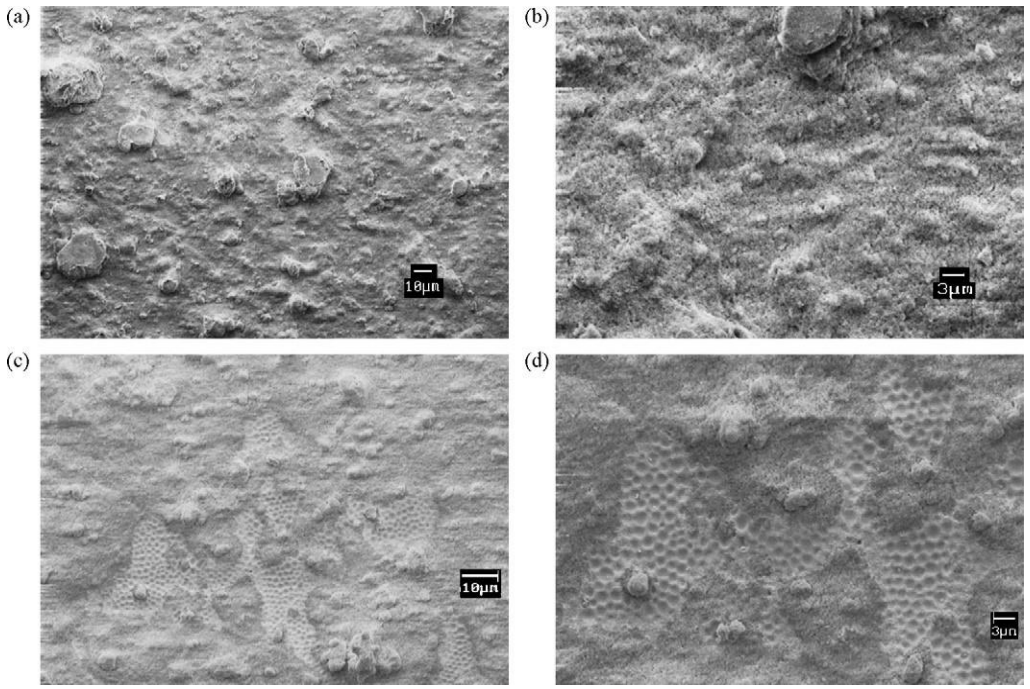

Fig. 6. SEM images of PVDF: HMFS (1:2) composite coatings prepared under different conditions (a) with freshly mixed precursor, 500X; (b) higher magnification of (a); (c) after ultrasonicating the precursor, 500; (d) higher magnification of (c) (Basu and Paranthaman, 2009).

ISSN: 0975-8585

Chakradhar et al (2014) studied the fabrication of stable PVDF-MWCNT composite SHB coatings by spray-coating method. The effects of CNT content and temperature on the SHCs were studied. In this paper, SHB was achieved by increasing the CNT content to 33.3 wt. % as shown in **Table 2**. Wettability is affected by surface microstructure, roughness and surface free energy. The authors have observed different wettability characteristics for different wt. % of MWCNTs in the PVDF matrix. In order to understand this phenomenon, surface morphology of the coatings was examined using FE-SEM. WCA of PVDF−10 wt. % MWCNT shows 122° with a SA of >90◦, and the corresponding FE-SEM images with different magnifications are shown in **Fig. 7**. As observed clearly from **Fig. 7** at lower MWCNT concentrations, the coatings have more porous structure. **Fig. 8** shows FE-SEM images of PVDF composite coatings with 33 wt. % MWCNT at different magnifications. With increase of MWCNT to 33 wt. %, the porosity slightly decreases with creation of protrusion like structures which can be clearly seen at higher magnifications, thereby increasing the WCA to 150° with SA ∼10◦. In general, the hydrophilic and hydrophobic coatings have lower average roughness (R_a) and root means square roughness (R_q), whereas the roughness is high for SHB coatings. Increasing MWCNT content to 66 wt. % leads to an enhanced surface roughness along with the creation of more protrusion like structures (**Fig. 9**). According to Cassie–Baxter's law, surface wettability changes with increasing WCA from 150° to 154° and with SA from ~10° to <3°. The higher WCA and lower SA at 66 wt. % MWCNT make these coatings SHB due to the creation of micro/nano-scale roughness.

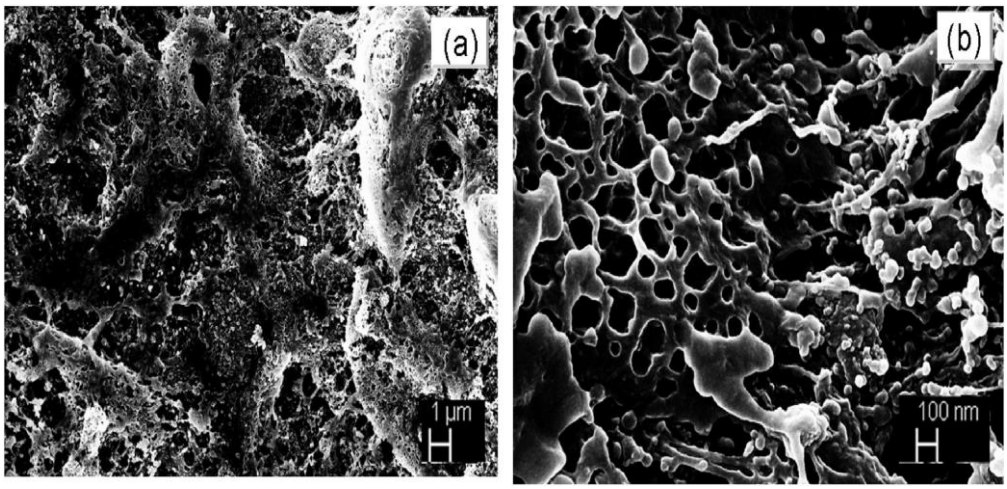

Fig. 7. FE-SEM images of PVDF–10 wt. % MWCNT at R.T. with different magnifications: (a) 5KX and (b) 50KX (Chakradhar et al., 2014).

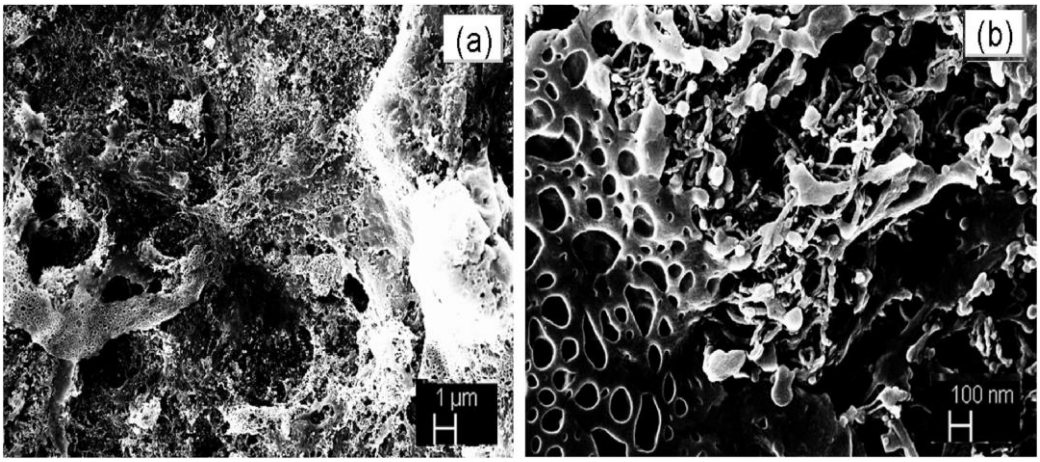

Fig. 8. FE-SEM images of PVDF–33 wt. % MWCNT at R.T. with different magnifications: (a) 5KX and (b) 50KX (Chakradhar et al., 2014).

ISSN: 0975-8585

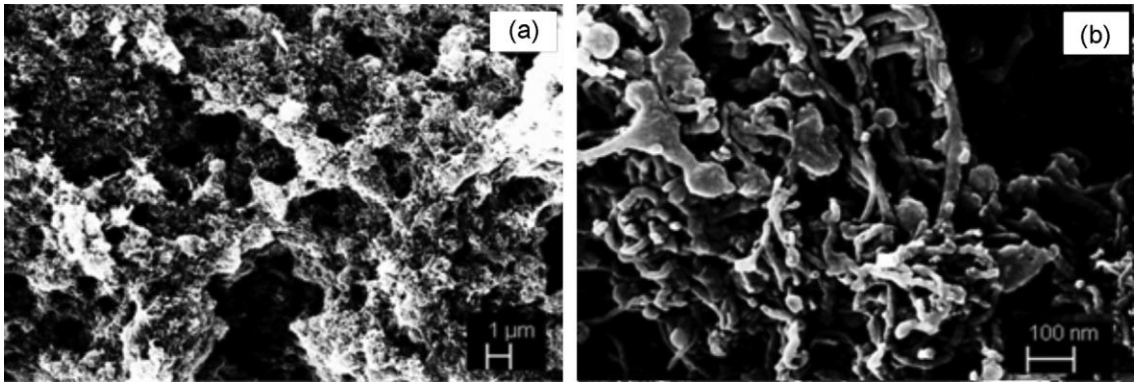

Fig. 9. FE-SEM images of PVDF–66 wt. % MWCNT at R.T. with different magnifications: (a) 5KX and (b) 50KX (Chakradhar et al., 2014).

Table 2: Compositions, WCA and SA of the coatings at R.T

S. No.	PVDF: MWCNT ratio	Content of MWCNT (wt. %)	WCA(◦)	SA1 (◦)	SA2 (◦)
1	10:0	0	105	>90	>90
2	9:1	10	122	>90	>90
3	4:1	20	131	>90	>90
4	3:1	25	133	>90	55
5	2:1	33.33	150	18	<10
6	1:1	50	152	10	<4
7	1:2	66.66	154	10	<3

Thermal stabilities of the PVDF–MWCNT SHB coatings were studied by heat treating the coatings at different temperatures (373, 423, 473, 523, 573, 623 K for 1 h), and measuring WCA after each treatment at R.T. WCA for the MWCNT (10 to 25 wt. %) containing films gradually decreases with temperature and reaches almost 10^{o} at 623 K. It is interesting to observe that, at 623 K, a transformation from SHB to SHL state is achieved (WCA < 10^{o}). The unusual wetting characteristics are governed by both chemical composition and the geometric microstructure of the surface. These studies suggest that the coatings are thermally stable up to 573 K exhibiting SHB behavior, and thereafter they transform to SHL state at 623 K.

Prasanth et al (2015) reported the synthesis of PVDF-ZrO_2 nanocomposite SHB coating. In this paper, nano ZrO_2 was synthesized from a new octa-coordinated metallo-organic complex of zirconium (IV) $[(CH_3COCHCOCH_3)_2Zr\{C_6H_4\ (N{=}CHC_6H_4O)_2\}]$. The mixture of PVDF and different concentrations (10, 20 and 30 wt. %) of nano ZrO_2 were dispersed in DMF and the solution was phase separated, and coated on a glass slide by using spray technique. Finally, these results were compared with the commercially available nano ZrO_2. From **Fig. 10(a–c)**, it is clear that WCA was increased with the addition of ZrO_2 nano-particles. The WCA values were 125, 136 and 153 for 10, 20 and 30 wt. % of nano-ZrO_2 in PVDF, respectively. Beyond 30 wt. %, there was no significant change in WCA. Therefore, they concluded that 30 wt. % was the optimal percentage to achieve SHB. The increase in the hydrophobicity might be due to dispersed nano-ZrO_2 particles responsible for increase in the micro–nano-roughness of the coating. In addition to this, they prepared the composite of 30 wt. % normal ZrO_2 (commercially available) in PVDF, and its coating showed WCA of 140^{o} (**Fig. 10d**).

Yan et al (2003) reported the synthesis of PVDF/$CaCO_3$ nanocomposite SHB coating. In this paper, PVDF is dissolved in DMF and further added 2 wt. % tridecafluoro octyltriethoxysilane and water. Finally, 1:1 ratio wt. % PVDF and $CaCO_3$ were drop-cast on the glass slide. The effect of stirring on morphology and CA were studied. The SEM image of pure PVDF coating made using the same solution casting method was displayed in **Fig. 11a**, showing even microspheres of 2.5 µm in diameter. **Fig. 11b and c** show the surface morphology of two PVDF/$CaCO_3$ coatings obtained with different stirring duration, 1 day and 3 days, respectively. Microspheres with a uniform size of around 4–5 µm are observed in **Fig. 11b**, and the surface of microspheres becomes rough and bump higher magnification. Microscopic differences in surface morphology exist between coatings of different stirring duration. With the long stirring period, the surface reveals some

ISSN: 0975-8585

smaller microspheres with a size of less than 1 µm, which are attached to the large microspheres, in **Fig. 11c**, while only a few smaller microspheres can be seen on the large ones for the coating with the short stirring period, in **Fig. 11b**. To test the dust removability, carbon black powder as dirt was deliberately spread on the PVDF/$CaCO_3$ coatings. It was found that the water droplet removed it easily when the coated surface has a slight tilt angle, the microscopic structures of the coatings shown and the droplet was finally covered with dirt, shown in **Fig. 11** are similar to those in crystalline polymer (**Fig. 12**), achieving the similar self-cleaning function of membrane systems including PVDF membrane.

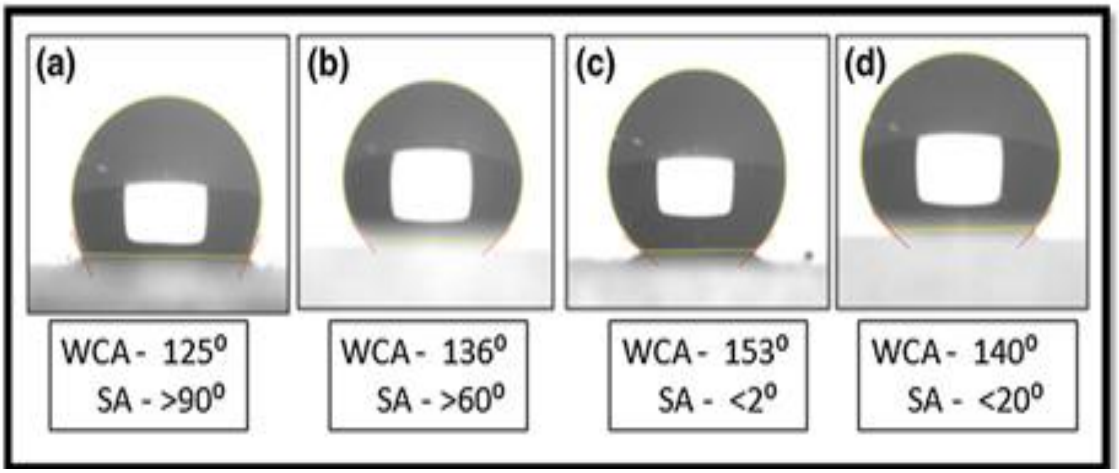

Fig. 10. WCA of PVDF–ZrO2 coatings with different ZrO2 concentrations of (a) 10 wt. % nano-ZrO2, (b) 20 wt. % nanoZrO2, (c) 30 wt. % nano-ZrO2, and (d) 30 wt. % normal ZrO2. (Prasanth et al. 2015).

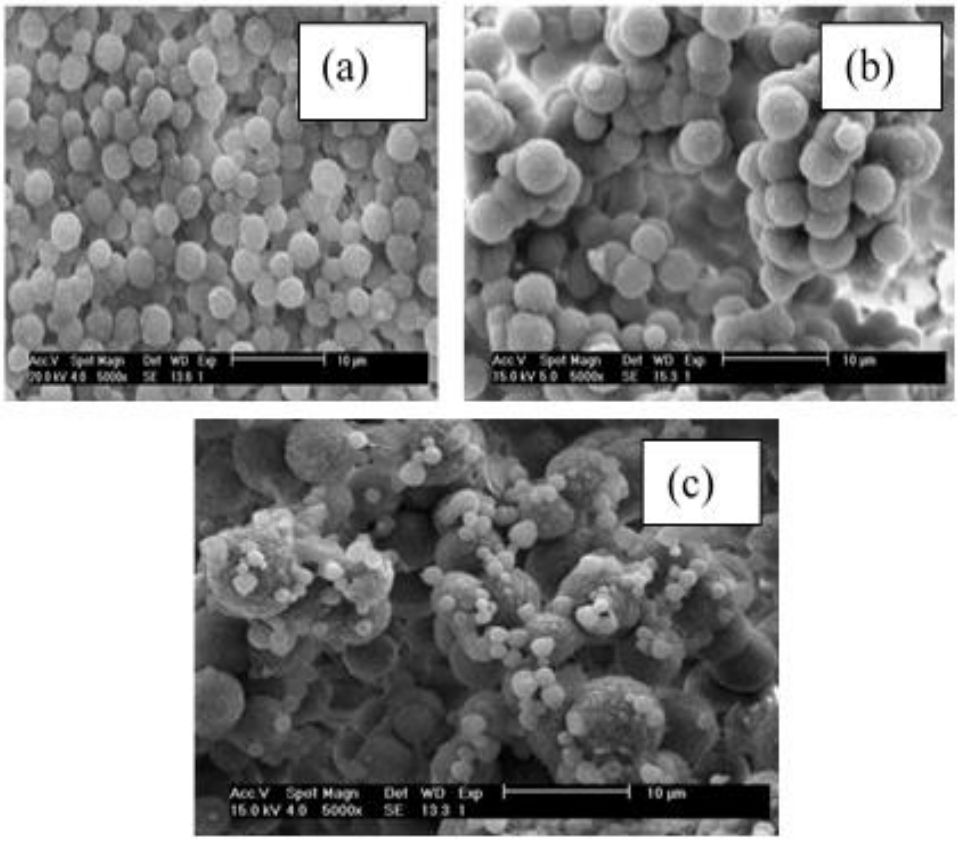

Fig. 11. SEM images of topological coating surfaces: (a) pure PVDF coating, (b) PVDF/CaCO3 coating with short stirring duration, and (c) PVDF/CaCO3 coating with long stirring duration (Yan et al. 2003).

ISSN: 0975-8585

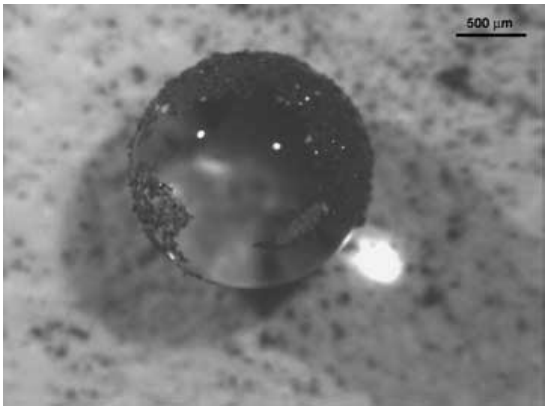

Fig. 12. Photograph of carbon black powder on PVDF/$CaCO_3$ coating removed by a water droplet (Yan et al. 2003).

SUMMARY AND FUTURE PROSPECTS

SHB is a fairly recent term used to describe the extreme water repellency of rough HB surfaces. HB fabrics, ultra-HB surfaces, water-resistant materials and SHB are among the most used terms in this field of research. The number and scope of techniques to generate SHB surfaces has greatly increased in recent years and along with that, new applications have also expanding with them. The main barrier preventing self-cleaning surfaces being used in many areas is that the surfaces are easily damaged or contaminated abrasive wear and washing cycles. Despite this, over 200 patents have been granted that use or produce SHB in some form or the other, and more new products are becoming commercially available. Some applications do not involve abrasion or contact with oils that may cause contamination, and have made use of these super-water-repellent surfaces. Communication and radar antennae and receivers are sometimes coated with SHB paint to reduce water/ice-induced distortion (e.g. Hirec by NTT-AT corp. Japan). With increasing researchers focusing in this field, the drawbacks are now well-understood and some can be minimized by choosing specific pathways to develop the SHB coatings. Potential applications of PVDF based SHB coatings have been proved and is found to be suitable for commercially viable large-area SHB coatings.

REFERENCES

[1] Balmert, A.; Bohn, H.F.; Ditsche-Kuru, P.; Barthlott, W. Dry under water: Comparative morphology and functional aspects of air-retaining insect surfaces. *J. Morph.* 2011, 272(4), 442–451.

[2] Barthlott, W.; Neinhuis, C. Purity of the sacred lotus, or escape from contamination in biological surfaces. *Planta* 1997, 202(1), 1−8.

[3] Basu, B.B.J.; Paranthaman, A.K. A simple method for the preparation of superhydrophobic PVDF–HMFS hybrid composite coatings. *Appl. Surf. Sci.* 2009, 255(8), 4479–4483.

[4] Bush, J.W.M.; Hu, D.L.; Prakash, M. The Integument of water-walking arthropods: Form and function. *Adv. Insect Physiol.* 2007. 34, 117–192.

[5] Celia, E.; Darmanin, T.; Givenchy, E.T. et al. Recent advances in designing super-hydrophobic surfaces. *J. Colloid Interface Sci.* 2013, 402(15), 1–18.

[6] Chakradhar, R.P.S.; Prasad, G.; Bera, P.; Anandan, C. Stable superhydrophobic coatings using PVDF–MWCNT nanocomposite. *Appl. Surf. Sci.* 2014, 301, 208–215.

[7] Feng, L.; Li, S. H.; Li, Y. S. et al. Super-hydrophobic surfaces: from natural to artificial. *Adv. Mater.* 2002, 14(24), 1857−1860.

[8] Hsieh, C.T.; Chang, B.S.; Lin, J.Y. Improvement of water and oil repellency on wood substrates by using fluorinated silica nanocoating. *Appl. Surf. Sci.* 2011, 257(18), 7997–8002.

[9] Lakshmi, R.V.; Bharathidasan, T.; Bera, P.; Basu, B. Fabrication of superhydrophobic and oleophobic sol-gel nanocomposite coating *J. Surf. Coat. Technol*. 2012, 206(19-20), 3888–3894.

[10] Madaeni, S.S.; Zinadini, S.; Vatanpour, V. Preparation of superhydrophobic nanofiltration membrane by embedding multiwalled carbon nanotube and polydimethylsiloxane in pores of microfiltration membrane. *Sep. Purif. Technol*. 2013, 111, 98–107, and references therein.

[11] Prasanth, V.G.; Prasad, G.; Kiran, T. et al. Synthesis, spectral characterization and crystal structure of a new precursor [$(CH_3COCHCOCH_3)_2Zr\{C_6H_4(N=CHC_6H_4O)_2\}$] for nano-zirconia: an investigation on the wettability of polyvinylidene fluoride–nano-zirconia composite material. *J. Sol-Gel Sci. Technol.* 2015,

76(1), 195-203.

[12] Wang, S.; Liu, K.; Yao, X.; Jiang, L. Bioinspired surfaces with superwettability: new Insight on theory, design, and applications. *Chem. Rev.* 2015, 115, 8230−8293.

[13] Watson, G.S.; Cribb, B.W.; Watson, J.A. How micro/nanoarchitecture facilitates anti-wetting: An elegant hierarchical design on the termite wing. *ACS Nano*, 2010, 4(1), 129–136.

[14] Xu, L.; Cai, Z.; Shen, Y.; Wang, L.; Ding, Y. Facile Preparation of superhydrophobic polyester surfaces with fluoropolymer/SiO_2 nanocomposites based on vinyl nanosilica hydrosols. *J. Appl. Polym. Sci.* 2014, 131(11), 40340, and references therein.

[15] Yan, L.; Wang, K.; Ye, L. Super hydrophobic property of PVDF/$CaCO_3$ nanocomposite coatings. *J. Mater. Sci. Lett.* 2003, 22, 1713–1717.